

[8] E. C. Jordan and K. G. Balmain, *Electromagnetic Waves and Radiating Systems*. Englewood Cliffs, N. J.: Prentice-Hall, 1968.
 [9] R. W. Beatty, "Calculated and measured S_{11} , S_{21} , and group delay for simple types of coaxial and rectangular waveguide 2-port standards," Nat. Bur. Stand. Tech. Note 657, Dec. 1974.

Performance Characteristics of 4-Port Stripline Circulators

ALI M. HUSSEIN, STUDENT MEMBER, IEEE,
 MAGDY M. IBRAHIM, MEMBER, IEEE, AND
 S. E. YOUSSEF

Abstract—Impedance matrix formulation is applied to the 4-port stripline circulator to determine the optimum performance. The space harmonics generated in the ferrite disk are determined. The distribution of the electric field and the power densities across the ferrite disk are clearly presented. Using an inner dielectric provides more flexibility in the design.

I. INTRODUCTION

The circulation adjustment of 4-port circulators cannot be reduced to an admittance matching procedure as in the 3-port case [1]. Three circulation conditions must be satisfied. Davies and Cohen [2] derived three equations describing the circulation conditions of a 4-port stripline circulator. Recently, Ku and Wu [3] have solved this problem by using Bosma's Green function method [4]. Several experimental studies were reported together with phenomenological description using the scattering matrix [1], [5], [6].

Here we use the impedance matrix formulation [7]–[9] to determine the circulation conditions and performance characteristics. To have a better insight into the circulation mechanism of the 4-port circulator, the space harmonics generated in the ferrite disk are determined. The field amplitude and the distribution of power densities across the ferrite disk are calculated. The effect of introducing an inner dielectric on the circulation conditions and performance is studied.

II. CIRCULATOR CHARACTERISTICS

Considering the boundary conditions for a symmetrical 4-port ferrite junction, the impedance matrix can be written in the form

$$\begin{bmatrix} E_1 \\ E_2 \\ E_3 \\ E_4 \end{bmatrix} = \begin{bmatrix} Z_1 & Z_2 & Z_3 & Z_4 \\ Z_4 & Z_1 & Z_2 & Z_3 \\ Z_3 & Z_4 & Z_1 & Z_2 \\ Z_2 & Z_3 & Z_4 & Z_1 \end{bmatrix} \begin{bmatrix} H_1 \\ H_2 \\ H_3 \\ H_4 \end{bmatrix} \quad (1)$$

where

$$Z_1 = jL \quad (2)$$

$$Z_2 = jM - K \quad (3)$$

Manuscript received October 16, 1974; revised June 23, 1975.

A. M. Hussein was with the Department of Electrical Engineering, Ain-Shams University, Cairo, Egypt. He is now with the Department of Electrical Engineering, University of Toronto, Toronto, Ont., Canada. M. M. Ibrahim and S. E. Youssef are with the Department of Electrical Engineering, Ain-Shams University, Cairo, Egypt.

TABLE I
 THE EFFECT OF VARYING ψ ON THE CIRCULATION CONDITION AND
 RELATIVE BANDWIDTHS

ψ°	k/μ	x	Z_e/Z_d	B.W. %	
				1-3	1-4
5	0.3166	3.795	1.0525	2.05	6.60
10	0.3105	3.780	0.5320	2.15	6.94
15	0.3055	3.759	0.3740	2.29	7.06

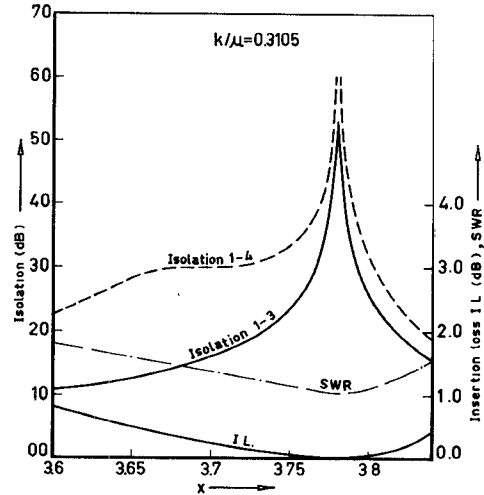


Fig. 1. Performance characteristics of a 4-port circulator. $k/\mu = 0.3105$, $Z_e/Z_d = 0.532$, and $\psi = 10^\circ$.

$$Z_3 = jN \quad (4)$$

$$Z_4 = jM + K \quad (5)$$

and where E_1 , E_2 , E_3 , and E_4 are the average values of the electric field at the four ports. The corresponding assumed constant values of the azimuthal component of the magnetic field are H_1 , H_2 , H_3 , and H_4 . K , L , M , and N are defined in [2]. Impedance matrix formulation has the advantage that it can handle easily externally tuned circulators [9].

Imposing the circulation condition (the ports 3 and 4 are completely isolated, and the input impedance is purely resistive and equals the wave impedance of the dielectric filling the striplines Z_d) on (1), three equations can be obtained [2]. These equations are solved considering up to the twelfth space harmonic. The computational results are given in Table I.¹ The table shows that as the stripline coupling angle ψ increases both the normalized radius x and the ratio k/μ decrease slightly. This is accompanied by a large decrease in the impedance ratio Z_e/Z_d . These results agree favorably with Ku and Wu [3].

The performance characteristics [isolation at ports 3 and 4, insertion loss, and standing-wave ratio (SWR)] are computed for $\psi = 10^\circ$, $k/\mu = 0.3105$, and $Z_e/Z_d = 0.532$ (Fig. 1). At $x = 3.78$ we have an ideal circulation (infinite isolation, zero insertion loss, and unity SWR). The relative 20-dB bandwidth for a 4-port circulator can be defined as the ratio of the band over which the isolation at ports 3 or 4 exceeds 20 dB to the central circulation frequency. Increasing ψ results in a small increase in the bandwidth at ports 3 and 4 (Table I). It is also shown that the isolation bandwidth at port 3 is less than that at port 4.

¹ The parameters ψ , k , μ , x , Z_e , and Z_d are defined in [2].

III. CIRCULATION MECHANISM

A. Space Harmonics

In the operation of a ferrite stripline circulator, many space harmonics are excited to satisfy the boundary conditions. The electric field across the ferrite disk can be written as follows [7]:

$$E_z(r, \phi) = \sum_{n=-\infty}^{\infty} a_n J_n(\alpha r) \exp(jn\phi) \quad (6)$$

where a_n is the space harmonic of the n th order. Table II shows the relative amplitudes of the space harmonics for the 4-port circulator at the circulation condition ($\psi = 10^\circ$). The table shows that they have nonnegligible amplitudes up to the tenth space harmonic. The zero mode has a relatively large value and consequently it greatly affects the circulation action. Thus, whereas a 3-port circulator can be described in terms of two counter rotating space harmonics (specifically, $n = \pm 1$ for $x = 1.84$) [7], a 4-port circulator is realized with the interaction of many space harmonics.

B. Field Distribution

The electric field and azimuthal component of the magnetic field are computed. The amplitude distribution of both fields at the periphery of the ferrite disk is shown in Fig. 2 at the circulation condition corresponding to $\psi = 10^\circ$ (Table I). The latter field has a smoother distribution than the assumed one and it fits the real situation [10]. The complete distribution of the electric field amplitude across the ferrite disk is shown in Fig. 3. It can be seen that the field amplitude at the center of the ferrite disk is strong. Hence the insertion of a central metal post will greatly disturb the circulation condition.

C. Power Density

The power densities in the radial and azimuthal directions are defined, respectively, as follows:

$$P_r = -\frac{1}{2} \operatorname{Re}(E_z H_\phi^*) \quad (7)$$

$$P_\phi = \frac{1}{2} \operatorname{Re}(E_z H_r^*). \quad (8)$$

TABLE II

THE RELATIVE AMPLITUDES OF THE SPACE HARMONICS FOR THE 4-PORT CIRCULATOR AT THE CIRCULATION CONDITION CORRESPONDING TO $\psi = 10^\circ$ (TABLE I)

$ n $	a_+	a_-	$ n $	a_+	a_-
0	6.87	~	7	0.34	0.34
1	0.05	0.02	8	0.20	0.10
2	1.53	3.12	9	0.42	0.10
3	9.15	2.06	10	0.34	0.17
4	1.12	0.35	11	0.12	0.13
5	1.50	0.29	12	0.07	0.04
6	1.03	0.46			

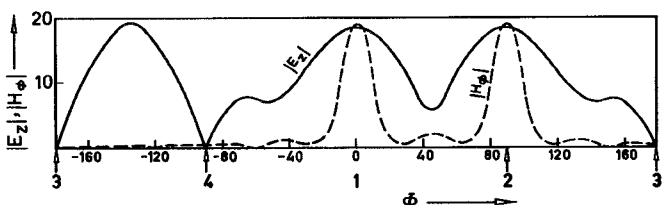


Fig. 2. The amplitudes of E_z and H_ϕ (to an arbitrary scale) along the periphery of the ferrite disk at the circulation condition, $\psi = 10^\circ$.

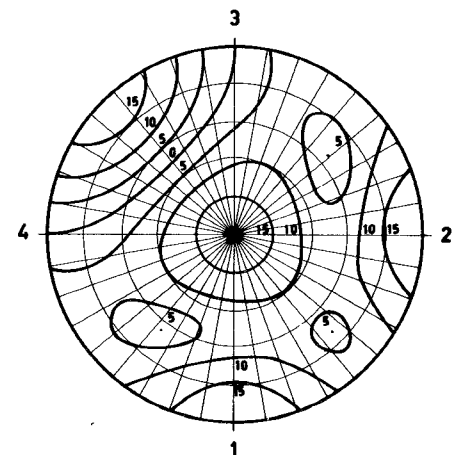
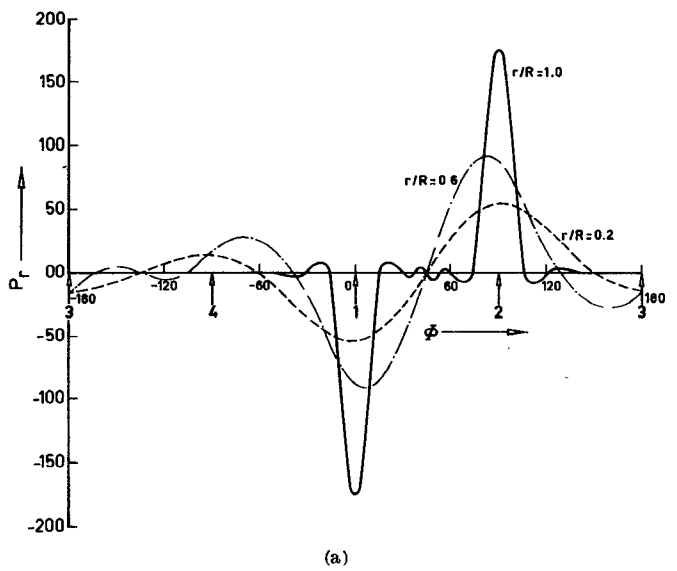
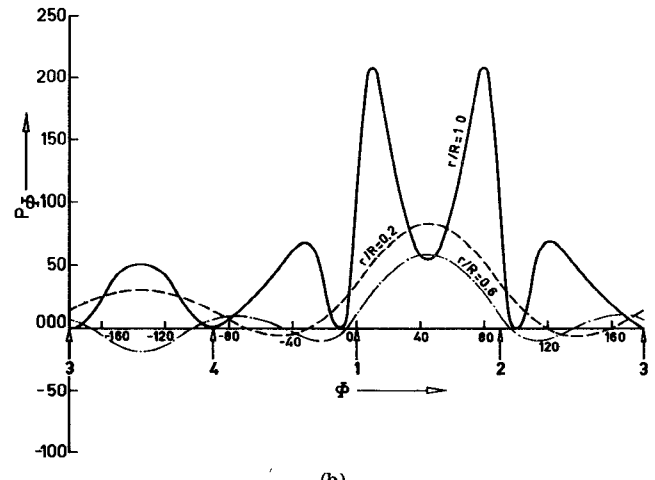


Fig. 3. The amplitude distribution of E_z (to the same scale as in Fig. 2) across the ferrite disk at the circulation condition, $\psi = 10^\circ$.



(a)



(b)

Fig. 4. The power-density distribution (to an arbitrary scale) across the ferrite disk for different radii at the circulation condition ($\psi = 10^\circ$). (a) The radial power density. (b) The azimuthal power density.

The power densities, at the circulation condition corresponding to $\psi = 10^\circ$, are plotted at three different radii ($r/R = 0.2, 0.6, 1$) in Fig. 4. Fig. 4(a) shows that the radial power density is nearly concentrated at ports 1 and 2 near the periphery of the ferrite disk. Going towards the center of the disk, the radial power density is gradually distributed over wider angles around ports 1 and 2. Fig. 4(b) shows that the azimuthal power density has a more complicated distribution. This can be justified by the corresponding complexity in the field distribution (Fig. 3). It can be noted that this power is nearly concentrated between ports 1 and 2.

The study of the power-density distribution gives a better insight into the power flow in the ferrite disk. It may be useful for circulators operating at high-power levels.

IV. INNER DIELECTRIC

Consider a central hole, inside the ferrite disk, filled with a dielectric material of permittivity ϵ_l and radius R_l . The z component of the electric field and the azimuthal component of the magnetic field in the dielectric and ferrite are, respectively, given by

$$E_z^{(1)}(r, \phi) = \sum_{n=-\infty}^{\infty} a_n^{(1)} J_n(\alpha_l r) \exp(jn\phi) \quad (9)$$

$$H_\phi^{(1)}(r, \phi) = jY_{el} \sum_{n=-\infty}^{\infty} a_n^{(1)} [J_n'(\alpha_l r) - (k/\mu) n J_n(\alpha_l r) / \alpha_l r] \cdot \exp(jn\phi) \quad (10)$$

$$E_z^{(2)}(r, \phi) = \sum_{n=-\infty}^{\infty} a_n^{(2)} [J_n(\alpha r) + \lambda_n Y_n(\alpha r)] \exp(jn\phi) \quad (11)$$

$$H_\phi^{(2)}(r, \phi) = jY_e \sum_{n=-\infty}^{\infty} a_n^{(2)} \{ [J_n'(\alpha r) - (k/\mu) n J_n(\alpha r) / \alpha r] + \lambda_n [Y_n'(\alpha r) - (k/\mu) n Y_n(\alpha r) / \alpha r] \} \exp(jn\phi) \quad (12)$$

where

$$\alpha_l^2 = \omega^2 \epsilon_0 \epsilon \mu_0 \quad (13)$$

$$Y_{el} = (\epsilon_0 \epsilon_l / \mu_0)^{1/2} \quad (14)$$

and

$$Y_e = 1/Z_e. \quad (15)$$

Matching the fields at the ferrite-dielectric boundary gives

$$\lambda_n = -[J_n'(\alpha R_l) - \gamma_n J_n(\alpha R_l)] / [Y_n'(\alpha R_l) - \gamma_n Y_n(\alpha R_l)] \quad (16)$$

where

$$\gamma_n = (Y_{el}/Y_e) [J_n'(\alpha_l R_l) / J_n(\alpha_l R_l) + (k/\mu) n / \alpha_l R_l \mu_0]. \quad (17)$$

Let

$$T_n(x) = J_n(x) + \lambda_n Y_n(x) \quad (18)$$

$$T_n'(x) = J_n'(x) + \lambda_n Y_n'(x). \quad (19)$$

Substituting $T_n(x)$ and $T_n'(x)$ in place of $J_n(x)$ and $J_n'(x)$, respectively, in the expressions of K , L , M , and N [2], modifies the circulation conditions to suit the inner dielectric case.

We consider the effect of changing the dielectric-ferrite radii ratio R_l/R and the permittivity ratio ϵ_l/ϵ on the circulation condition and the performance. Fig. 5 shows the dependence of the normalized radius x , k/μ , and Z_e/Z_d , for an ideal circulation, on R_l/R . The figure is plotted for three different values of ϵ_l/ϵ (0.5, 1, 2).

The performance characteristics are computed and from which the isolation 20-dB bandwidths are determined. Fig. 6 shows the variation of the relative bandwidths (1-3, 1-4) with respect to the ratio R_l/R .

Hence using an inner dielectric would not only improve the power capability of the circulator [7], [8], [11], but provides more flexibility in the design as well.

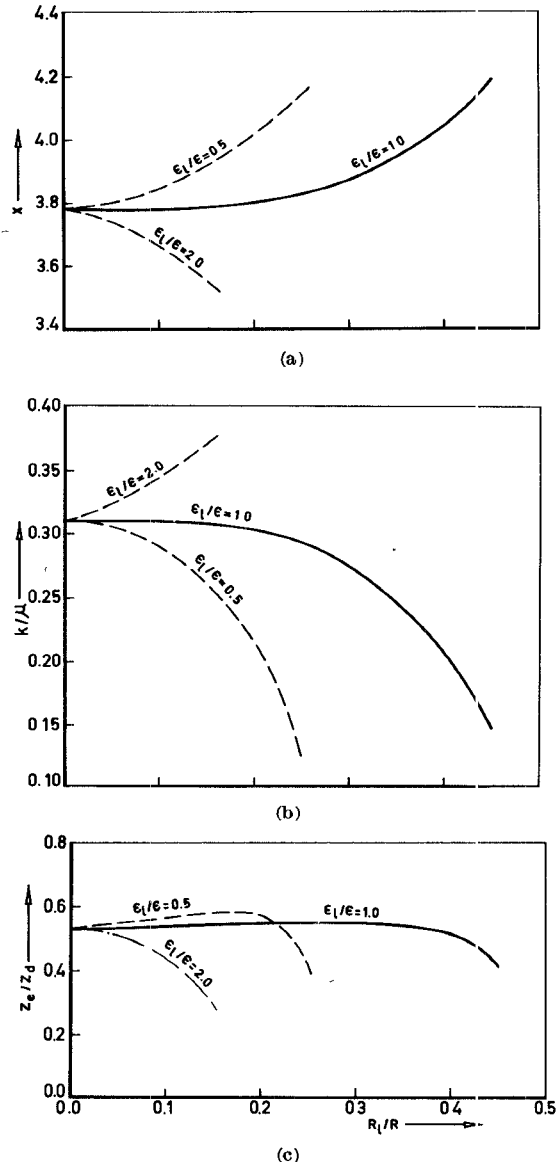


Fig. 5. The dependence of the circulator parameters on R_l/R for different values of ϵ_l/ϵ (0.5, 1, 2). $\psi = 10^\circ$. (a) The normalized radius x . (b) The ratio k/μ . (c) The impedance ratio Z_e/Z_d .

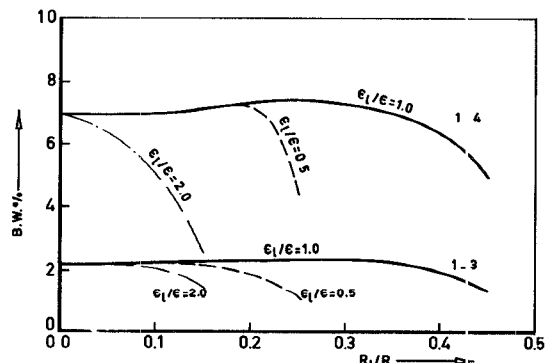


Fig. 6. The variation of the relative bandwidths (1-3, 1-4) as functions of R_l/R for different values of ϵ_l/ϵ . $\psi = 10^\circ$.

V. CONCLUSIONS

Using the impedance matrix formulation, the circulator parameters and performance characteristics are determined. The relative bandwidth at port 3 is less than that at port 4. These bandwidths increase slightly with increasing the stripline coupling angle.

A 4-port circulator is realized by the interaction of many space harmonics. The zero mode has a relatively large value and consequently it greatly affects the circulation action. The electric field at the center of the ferrite disk is strong. Therefore, the insertion of a central metal post will greatly disturb the circulation condition.

The study of the power-density distribution may be useful for circulators operating at high-power levels. It is noticed that the power is mainly concentrated near and between ports 1 and 2.

An inner dielectric would not only improve the power capability of the circulator, but would provide more flexibility in the design as well.

REFERENCES

- [1] J. Helszajn and C. R. Buffler, "Adjustment of the 4-port single junction circulator," *Radio Electron. Eng.*, vol. 35, pp. 357-360, June 1968.
- [2] J. B. Davies and P. Cohen, "Theoretical design of symmetrical junction stripline circulators," *IEEE Trans. Microwave Theory Tech.*, vol. MTT-11, pp. 506-512, Nov. 1963.
- [3] W. H. Ku and Y. S. Wu, "On stripline four-port circulator," in *IEEE Int. Microwave Symp. Dig.*, IEEE Cat. 73, 737-9, pp. 86-88, 1973.
- [4] H. Bosma, "On stripline Y-circulation at UHF," *IEEE Trans. Microwave Theory Tech.*, vol. MTT-12, pp. 61-72, Jan. 1964.
- [5] C. E. Fay and W. A. Dean, "The 4-port single junction circulator in stripline," in *G-MTT Symp.*, pp. 286-289, Sept. 1966.
- [6] J. Helszajn, "Waveguides and stripline 4-port single junction circulators," *IEEE Trans. Microwave Theory Tech. (Short Papers)*, vol. MTT-21, pp. 630-633, Oct. 1973.
- [7] H. Bosma, in *Advances in Microwaves*, vol. 6, L. Young, Ed. New York: Academic, 1971.
- [8] J. Helszajn, "Composite-junction circulators using ferrite disks and dielectric rings," *IEEE Trans. Microwave Theory Tech.*, vol. MTT-22, pp. 400-410, Apr. 1974.
- [9] R. H. Knerr, C. E. Barnes, and F. Bosch, "A compact broad-band thin-film lumped-element L-band circulator," *IEEE Trans. Microwave Theory Tech. (1970 Symposium Issue)*, vol. MTT-18, pp. 1100-1108, Dec. 1970.
- [10] Y. S. Wu and F. J. Rosenbaum, "Wide-band operation of microstrip circulators," *IEEE Trans. Microwave Theory Tech.*, vol. MTT-22, pp. 849-856, Oct. 1974.
- [11] J. Helszajn, "A ferrite ring stripline junction circulator," *Radio Electron. Eng.*, vol. 32, pp. 55-60, July 1966.

tion loss of the junction. One application of this arrangement is encountered in the connection of a filter and equalizer by a single circulator. The final result indicates that, in the absence of circuit losses, the double path loss varies between one and three times the single path loss.

The insertion loss of a 3-port circulator between ports 1 and 3 with port 2 terminated in a variable short circuit is of some interest in a number of situations. One such application is where a circulator is used to connect a filter and an equalizer. Another application is in phasors using circulators with one port terminated in a p-i-n diode switch. The insertion loss of such an arrangement has been studied in [1] and [2], in terms of the elements of the *Q*-matrix. The purpose of this short paper is to give approximate upper and lower bounds on the loss in terms of the single path loss L_0 of the circulator.

The exact relation is given in [1] by

$$L = \frac{P_a}{P_i} = X(1 + S_{21}^2) - 2YS_{21} \cos(\eta - \Psi_1 + \Psi_2) \quad (1)$$

where L is the total insertion loss between ports 1 and 3, P_i and P_a are the total incident and dissipated powers, S_{21} is the usual transmission coefficient between ports 1 and 2, $\Psi_{1,2}$ are the phase angles of the input waves at ports 1 and 2, X and $Ye^{i\eta}$ are the entries of the *Q*-matrix, and X represents the single path insertion loss of the circulator between ports 1 and 2. Fig. 1 depicts the schematic studied in this text. Some simplification of the preceding relation is possible by relating X , Y , and S_{21} through the eigenvalues of the *Q*-matrix [3].

The result is

$$X \approx \frac{2q_1}{3} \quad (2)$$

$$Y \approx \frac{q_1}{3} \quad (3)$$

$$S_{21} \approx 1 - \frac{q_1}{3} \quad (4)$$

$$\eta = 0 \quad (5)$$

provided

$$S_{11} \approx S_{12} \approx 0 \quad (6)$$

where q_1 is the dissipation eigenvalue of the demagnetized counter-rotating eigennetworks.

It is observed that $X = 2Y$ is consistent with the example given by Hagelin in [1].

The preceding approximations omit the dissipation of the in-phase

Insertion Loss of 3-Port Circulator with One Port Terminated in Variable Short Circuit

J. HELSZAJN, MEMBER, IEEE,
GORDON P. RIBLET, MEMBER, IEEE,
AND J. R. MATHER

Abstract—The insertion loss between ports 1 and 3 of a 3-port circulator with port 2 terminated in a short circuit varies about twice the single path loss. The purpose is to give approximate simple upper and lower bounds for this loss in terms of the single path inser-

Manuscript received March 3, 1975; revised June 25, 1975.

J. Helszajn is with the Department of Electrical and Electronic Engineering, Heriot-Watt University, Edinburgh, Scotland.

G. P. Riblet is with the Microwave Development Laboratories, Needham Heights, Mass. 02194.

J. R. Mather is with Ferranti Limited, Italy.

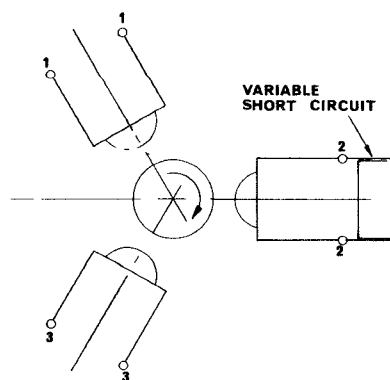


Fig. 1.